BNL-210861-2019-TECH

C-A/AP/616

Improving the luminosity for Beam Energy Scan II at RHIC

C. Liu

January 2019

Collider Accelerator Department

Brookhaven National Laboratory

U.S. Department of Energy

USDOE Office of Science (SC), Nuclear Physics (NP) (SC-26)

DISCLAIMER

Improving the luminosity for Beam Energy Scan II at RHIC

C. Liu[*], M. Blaskiewicz, K.A. Drees, A.V. Fedotov, W. Fischer, C.J. Gardner, H. Huang, D. Kayran, Y. Luo, G. Marr, A. Marusic, K. Mernick, M. Minty, C. Montag, I. Pinayev, S. Polizzo, V. Ranjbar, D. Raparia, G. Robert-Demolaize, T. Roser, J. Sandberg, V. Schoefer, T. Shrey, S. Tepikian, P. Thieberger, A. Zaltsman, K. Zeno, I. Zhang, W. Zhang,
Brookhaven National Lab, Upton, NY, USA.

January 7, 2019

[*]cliu1@bnl.gov

1 Introduction

The QCD (Quantum Chromodynamics) phase diagram [1], one of the most important graphs in nuclear physics, has many uncharted territories. In particular, the nature of the transformation from Quark-Gluon plasma (QGP) to the state of Hadronic gas is totally unknown [2]. A beam energy scan [3, 4], scanning the phase diagram with variable collision energy, has been conducted at RHIC to explore the first-order phase transition and determine the location of a possible critical point. The beam energy scan I (BES-I) [5] was completed in 2014 and resulted in improved understanding of many physics phenomena [6]. However, the transition between QGP and hadronic gas has not been understood yet. BES-I program offered a limited statistics because the RHIC luminosity decreases steeply at lower energies. Therefore, the beam energy Scan II (BES-II) is planned with luminosity improved by a factor of ~ 4 at the same beam energies as BES-I (3.85, 4.55, 5.75, 7.3 and 9.8 GeV/nucleon).

The beam lifetime at BES-I energies was limited by some physical effects [7, 8, 9], of which the most significant are intrabeam scattering, space charge, beam-beam, and persistent current effects. These effects have been understood better through beam operation in BES-I and beam studies over the years [7, 10, 11, 12]. Corresponding countermeasures [13, 14, 15, 16, 17, 18, 19] for these physical effects have been either conceived or tested before the start of BES-II. This note reviews the physical effects that limit beam lifetime therefore luminosity, and introduces the countermeasures which will be in place to improve BES-II luminosity.

2 Intrabeam scattering and electron cooling

2.1 Intrabeam scattering

At BES-I/II beam energies, which are below the transition energy ($\sim$24 GeV/nucleon for Au beam), both longitudinal and transverse beam emittance grow rapidly due to intrabeam scattering (IBS) [20, 18], the small angle scattering process between the particles in a bunched or a coasting beam.

Table 1: IBS induced longitudinal beam emittance growth time ($\tau_{\|}$) and transverse ($\tau_{\perp}$) beam emittance growth time at BES-I/II beam energies with 28 MHz cavities and 9 MHz cavities.

Energy	28 MHz cavities			9 MHz cavities		
(GeV/nucleon)	$N_{ppb}(10^9)$	$\tau_{\|}$(mins)	$\tau_{\perp}$(mins)	$N_{ppb}(10^9)$	$\tau_{\|}$(mins)	$\tau_{\perp}$(mins)
3.85	0.5	18	43	0.6	20	117
4.55	0.5	28	63	0.8	19	134
5.75	1.1	14	28	1.3	20	131
7.3	1.8	33	49	2.1	14	142
9.8	2.1	56	77	2.3	15	150

The luminosity lifetime was mostly limited by the IBS effect during BES-I operation [13]. The IBS beam emittance growth times at BES-I/II beam energies, calculated using BETACOOL [21], range from ten minutes to tens of minutes as shown in Table 1. The bunch intensities are different when using the 28 or 9 MHz cavities due to the difference in longitudinal acceptance of the two RF systems. The 28 MHz cavities were used for all beam energies during BES-I operation. Three new 9 MHz cavities per accelerator [22] will be used for the three lowest energies during BES-II operation.

2.2 Low Energy RHIC electron Cooling

The Low Energy RHIC electron Cooling (LEReC) [23], using a linear electron accelerator (Figure 1), is designed to combat the IBS effect by cooling RHIC ion beams, and therefore to improve luminosities at the three lowest beam energies. Electron bunches are generated by a 400 kV DC electron photocathode gun [24]; these bunches then go through a chain of cavities, which includes a 1.2/1.6/2.2 MeV 704 MHz superconducting booster cavity, a 2.1 GHz normal-conducting copper cavity to linearize the beam energy chirp, a 704 MHz normal-conducting cavity to reduce the energy spread of individual bunches and a 9 MHz normal-conducting cavity to reduce the energy droop along a bunch train due to beam loading. Each electron macro-bunch, consisting of 30 micro-bunches of 40 ps length at 704 MHz repetition frequency, will overlap with a RHIC ion bunch at 9 MHz frequency. The electron beam first co-propagates with the ion beam in one of the RHIC rings (Yellow) at the same velocity, then turns around and co-propagates with the ion beam in the other RHIC ring (Blue). With its small energy spread (5×10^{-4}), the electron beam reduces the ion beam energy spread when interacting with it by coulomb friction force. The design electron beam current is 30 mA for a beam energy of 2.0 MeV and 35 mA for a beam energy of 2.6 MeV, with bunch charges of 130-200 pC and a normalized emittance of 2.5 μm.

All the Key Performance Parameters of the LEReC project have been demonstrated [25, 26] as of Sep. 2018 and LEReC is transitioning towards operations. LEReC cooling commissioning is planned for 2019; operation of LEReC is expected in 2020.

3 Space charge and RF cavities

3.1 Space charge

At the BES-I/II beam energies, the ions in the beam experience a strong direct space charge force. The space charge force introduces incoherent and coherent tune shifts. As a result, the high intensity beam can be driven to low-order resonances which deteriorate beam lifetime. The incoherent space charge tune shift [27] of a Gaussian beam from direct space charge in a circular ring can be

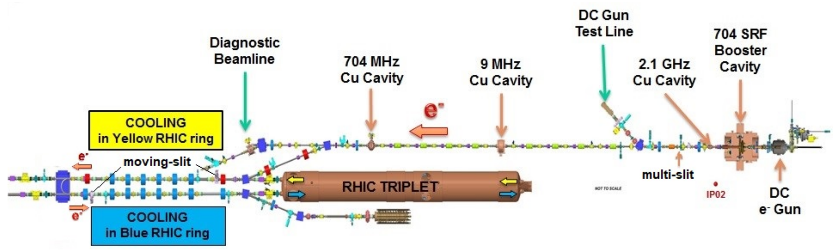

Figure 1: Schematics of Low Energy RHIC electron Cooling accelerator. Low energy electron beam is transported through a beamline with solenoids, merged into a cooling section in the Yellow RHIC ring first, turned around and merged into a cooling section in the Blue RHIC ring.

estimated by

$$\delta Q_{sc} = -\frac{r_0}{4\pi}\frac{Z^2}{A}\frac{N}{\beta\gamma^2\epsilon_n}\frac{F}{B_f} \tag{1}$$

where r_0 is the classical radius of proton, Z and A are the charge number and atomic number, N is the number of particles per bunch, β and γ are the relative velocity and relativistic factor, ϵ_n is the RMS normalized transverse emittance, F (~ 1) is the form factor due to image current space charge force, $B_f = \frac{2\pi R}{\sqrt{2\pi}\sigma_s}$ is the bunching factor, and σ_s is the RMS bunch length.

3.2 RF cavities

Three new 9 MHz cavities (with 180 kV total voltage, the harmonic number h=120) will be used for the three lowest beam energies during BES-II operation. The 28 MHz cavities (with 400 kV total voltage, the harmonic number h=360) are kept for operation at the two higher beam energies. The incoherent space charge tune shifts at BES-I/II beam energies with different RF cavities are shown in Table 2. The space charge effects are significantly reduced by using the new 9 MHz cavities due to reduced peak beam intensity.

Table 2: Space charge incoherent tune shifts (δQ_{sc}) at BES-I/II beam energies with 28 MHz cavities and 9 MHz cavities.

Energy (GeV/nucleon)	28 MHz cavities		9 MHz cavities	
	$N_{ppb}(10^9)$	δQ_{sc}	$N_{ppb}(10^9)$	δQ_{sc}
3.85	0.5	0.073	0.6	0.038
4.55	0.5	0.053	0.8	0.037
5.75	1.1	0.072	1.3	0.039
7.3	1.8	0.072	2.1	0.044
9.8	2.1	0.049	2.3	0.032

The frequency range of these 9 MHz cavities is from 8.7 to 9.6 MHz [22].

With this frequency range, the harmonic number of these cavities for BES-II beam energies can stay constant at 120, thus avoiding a change of the harmonic number which was mandatory with 28 MHz cavities [28]. A minor downside of using these new 9 MHz cavities is that the longitudinal IBS growth rates become stronger due to a smaller energy spread. The 28 MHz cavities will be employed in addition to increase the beam energy spread therefore alleviating the IBS effect at 5.75 GeV/nucleon for which the LEReC cooling may not be available.

The 9 MHz cavities provide a larger bucket area than the 28 MHz cavities as shown in Table 3. Therefore, bunch intensities can be increased for the three lowest beam energies during BES-II. For beam energies at 9.8 and 7.3 GeV/nucleon, the 28 MHz cavities will be used during operation for better luminosity lifetime even though its longitudinal acceptance is smaller than that of the 9 MHz cavities [29].

Table 3: Longitudinal bucket area at BES-I/II beam energies with 28 MHz cavities and 9 MHz cavities.

Energy (GeV/nucleon)	28 MHz cavities bucket area (eV·s)	9 MHz cavities bucket area (eV·s)
3.85	0.17	0.60
4.55	0.23	0.80
5.75	0.34	1.18
7.3	0.51	1.77
9.8	0.85	2.96

3.3 Injection and extraction kicker

Longer bunches ($\sim$ 50 ns full length) are expected with 9 MHz cavities. Therefore, the requirement of the extraction kicker in AGS and the injection kicker in RHIC [30] are more demanding [31] for BES-II operation. In general, a longer flattop of the voltage pulse is desired for both kickers to avoid significant emittance growth; a short rise time is also required as to not affect the preceding bunch. With less strength required from the AGS extraction kicker at low energies, the four kicker pulses can be stacked for a longer and flatter top. The rise time of the AGS extraction kicker is 175 ns which is short enough to extract equidistantly spaced 6 bunches in one cycle. The rise time was shortened and the flattop was extended for the RHIC injection kicker by switching from the previous setup with 40 Ω termination to a setup with 25 Ω termination. The measurements [32] with the new setup demonstrated the specifications of the RHIC injection kicker required for operation with 9 MHz cavities.

4 Beam-beam and working point

4.1 Beam-beam effects

With the upgrade of PHENIX to sPHENIX in progress, beams will only collide at IP6 for the STAR experiment during the BES-II program. During beam collisions, particles in one beam experience the electric and magnetic forces from the particles in the other beam. The nonlinear beam-beam force excites nonlinear resonances and creates an amplitude dependence of the betatron tune [33]. The strength of the beam-beam force is characterized by the incoherent beam-beam tune shift [33], which can be estimated by

$$\xi = -\frac{Z^2 N r_0}{4\pi A \epsilon_n} \tag{2}$$

where the notations are the same as used in Eq. 1.

Even though the incoherent beam-beam tune shifts at BES-I/II beam energies, listed in Table 4, are small, a significant impact on beam lifetime with collisions was observed during BES-I operation [15]. The impact was attributed to the interplay of beam-beam and the space charge effects, and was reproduced in simulation [34]. To improve the beam lifetime with collisions, a new near-integer working point (0.098/0.095), with more tune space for the space charge and beam-beam tune shift, was proposed. Beam experiments demonstrated that beam lifetime was much less affected [15] when beam collisions were established.

Table 4: Beam-beam incoherent tune shifts at BES-I/II beam energies with 28 MHz cavities and 9 MHz cavities.

Energy	28 MHz cavities	9 MHz cavities
(GeV/nucleon)	Tune shift (10^{-3})	Tune shift (10^{-3})
3.85	1.0	1.1
4.55	1.0	1.5
5.75	2.1	2.5
7.3	3.5	4.0
9.8	4.1	4.4

4.2 Working point

The new working point (0.098/0.095), proposed for BES-II beam energies, was tested at 13.5 GeV/nucleon beam energy [35]. We observed substantially reduced beam loss shortly after collisions being established. However, the orbit rms was not successfully suppressed to <mm level by orbit feedback with the new working point. This problem was attributed to the reduced resolution of corrector power supplies at low beam energies and optics errors. All the corrector power supply controllers are being upgraded from 12 to 16 bit to better control the orbit; and optics correction is also planned for BES-II operation.

5 Persistent current and new magnetic cycle

5.1 Persistent current effects

Persistent currents in superconducting magnets introduce significant field errors [36] especially at low operating currents; in addition, their decay cause variations of beam parameters, like orbit, tune and chromaticity [37]. The sextupole component in RHIC dipoles was so strong that the polarity of some sextupole magnets were flipped just to be able to compensate the natural and field errors induced chromaticities [38]. To deal with the persistent current decay, the operators waited for about 2 hours for the magnets to settle down before beam operation at fixed magnetic fields commenced. The magnets were kept at constant operating currents for an extended time period, however, interruption of operation did happen due to quench-link interlocks and electric failures. With LEReC commissioning at 3.85 GeV/nucleon and RHIC operation at 9.8, 7.3 and 31.2 GeV/nucleon in 2019, the beam energy will be switched back and forth on a daily basis so that quick establishment of stable machine conditions is extremely important. To reduce field errors and quickly establish stable machine conditions, new magnetic cycles [39] were proposed for all BES-II beam energies.

5.2 New magnetic cycle

The conventional magnetic cycle for beam operation at 9.8 GeV/nucleon is shown in Figure 2. In the new magnetic cycle for 9.8 GeV/nucleon, the magnet current oscillates around the operating current with diminishing amplitude a couple of times before it settles (Figure 3). This new magnetic cycle has been demonstrated experimentally to reduce field errors and establish stable machine conditions in 10-20 minutes [40]. New magnetic cycles will be designed for operation at all BES-I/II beam energies.

6 Lattice design

With reduced field errors and improved machine stability, smaller beta star values at interaction point 6 (IP6) for BES-II than those previously used for BES-I are being considered to increase the luminosity. The beta star values for BES-I (β_o^*) and the beta star values being considered for BES-II (β_n^*) are listed in Table 5. These new beta star values were proposed with consideration of the aperture limit in the final focusing quadrupoles near IP6 (110 mm diameter). $\sigma_{triplet}$ is the RMS beam size at the final focusing quadrupole calculated with the newly proposed beta star values and the normalized RMS transverse beam emittance ($\epsilon_{n,rms}$), which was conservatively assumed as 3.5 μm at all BES-II beam energies at the end of the physics store based on previous measurements.

The beta functions at the cooling section, located in sector-1 and $\sim$ 40-58 m from IP2, are required to be close to uniform in the range of 25 to 50 m for

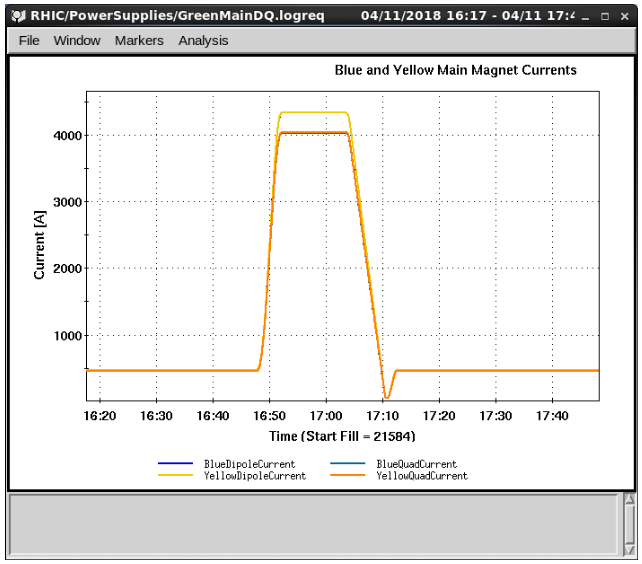

Figure 2: The old magnetic cycle: RHIC dipoles (and quadrupoles) were ramped to 4334 A, back down to 50 A, then up to 473.3 A for beam injection.

Table 5: The beta star values used for BES-I and the beta star values proposed for BES-II.

Energy (GeV/nucleon)	$\epsilon_{n,rms}(\mu m)$	β_n^*(m)	$\sigma_{triplet}$(mm)	β_o^*(m)
3.85	3.5	4.0	16.9	6.0
4.55	3.5	3.5	16.5	10.0
5.75	3.5	2.5	17.3	6.0
7.3	3.5	2.0	17.1	3.5
9.8	3.5	1.5	17.0	3.0

matching the transverse profiles of electron and Au beam.

To match the velocity of electron and Au beam for cooling, special design lattices are needed for recombination monitoring [41, 42, 43] at beam energies of 3.85, 4.55 and 5.75 GeV/nucleon. A lattice was designed with a working point at 0.11/0.13 so far with no consideration of the cooling section requirement [44]. The effort of lattice design is still in progress.

7 Injector beam parameters

The injector beam parameters, especially the longitudinal emittance and intensity, is limited/defined by the longitudinal acceptance of RHIC. The longitudinal acceptances of RHIC at various beam energies are listed in Table 3.

Beam studies were carried out in the injectors, mostly the AGS, to finalize

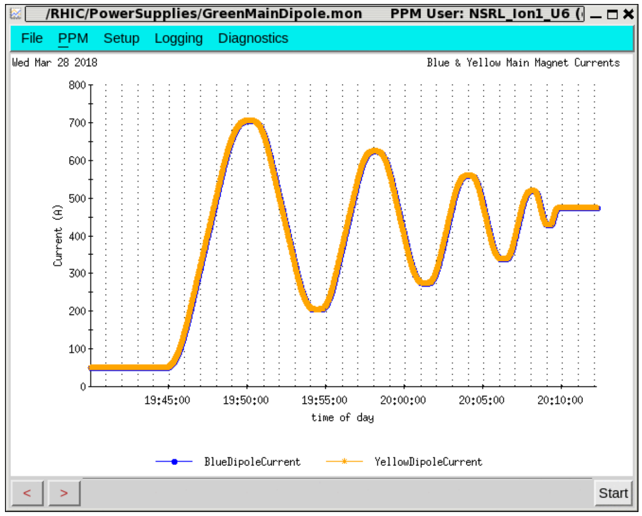

Figure 3: The new magnetic cycle: RHIC dipoles (and quadrupoles) were ramped up and down several times, with intermediate current points at [50, 700, 200, 625, 275, 560, 340, 520, 430] A, before being held constant at 473.3 A for beam injection.

beam parameters with the constraint of the RHIC longitudinal acceptance in mind. The beam parameters [45], which are suggested to be used for BES-II, are selected and listed in Table 6.

Table 6: Measured longitudinal emittance and bunch intensities in AGS at BES-I/II beam energies during beam studies in 2018.

Energy (GeV/nucleon)	bucket area (eV·s)	Merge scheme	Long. emitt (eV·s)	N_{ppb} (10^9)	# of bunches
3.85	0.6	2→1	0.29	0.8	6
4.55	0.8	6→3→1	0.32	1.34	2
5.75	1.18	6→3→1	0.39	1.7	2
7.3	0.51	6→3→1	0.71	2.3	2
9.8	0.85	6→3→1	0.78	2.3	2

The # of bunches is the number of bunches that can be provided in one AGS cycle. A large number of bunches per AGS cycle has the advantage of shortening the injection time in RHIC. The bunch intensities can be further increased at the three lowest beam energies since the bucket area with 9 MHz is larger than the longitudinal beam emittance. The bucket area at 7.3 GeV/nucleon is the smallest therefore beam operation with limited bunch intensity ($\sim 1.8 \times 10^9$ ppb) is expected.

8 Beam parameters and projections

The expected beam parameters in RHIC [31] and the projected luminosities [46] at low beam energies are listed in Table 7. The luminosities at the three lowest beam energies are expected to be kept almost constant during the course of physics stores with LEReC electron cooling engaged.

Table 7: Beam parameters and luminosity projections for BES-II.

Parameter	Unit	3.85 GeV	4.55 GeV	5.75 GeV	7.3 GeV	9.8 GeV
γ		4.135	4.887	6.175	7.840	10.525
$B\rho$		31.07	37.40	47.20	60.23	81.11
f_{cavity}	MHz	9.104984	9.184964	9.259703	27.9203	28.02288
V_{cavity}	kV	180	180	180	400	400
A_{bucket}	eV·s	0.6	0.8	1.18	0.51	0.85
ϵ_s	eV·s	0.35	0.43	0.6	0.5	0.75
N_{ppb}	10^9	0.6	0.8	1.3	1.8	2.1
n_b		111	111	111	111	111
β^*	m	6	6	5	3.5	3
L_{peak}	$10^{24}cm^{-2}s^{-1}$	8.1	17.2	70.2	246.60	529.5
L_{ave}	$10^{24}cm^{-2}s^{-1}$	5.0	15.0	60.0	60.0	132.0

9 Summary

This note summarized the challenges for BES-II operation planned in year 2019-2020/21 at RHIC, and introduced the countermeasures to overcome these challenges. The new working point for alleviating the interplay of beam-beam and space charge effects, the new magnetic cycles for combating persistent current effects and smaller beta star values for smaller beam sizes at the collision point, are expected to help improve the luminosities at all beam energies. At beam energies 9.8 and 7.3 GeV/nucleon, the luminosity goals will be achieved with these measures alone and without electron cooling being implemented. At the three lowest and most challenging beam energies (5.75, 4.55 and 3.85 GeV/nucleon), the 9 MHz cavities will be used for reducing space charge effects; and more critically, LEReC electron cooling is expected to be operational so that the luminosity goals can be achieved.

References

[1] M. Stephanov. QCD phase diagram and the critical point. *International Journal of Modern Physics A*, 20(19):4387–4392, 2005.

[2] M. Stephanov, K. Rajagopal, and E. Shuryak. Signatures of the tricritical point in QCD. *Physical Review Letters*, 81(22):4816, 1998.

[3] Can we discover QCD critical point at RHIC. RIKEN BNL Research Center Report No. BNL-75692-2006.

[4] G. Stephans. critRHIC: the RHIC low energy program. *Journal of Physics G: Nuclear and Particle Physics*, 32(12):S447, 2006.

[5] C. Montag and A. Fedotov. RHIC low energy acceleration. In *Proc. of CPOD2013*, page 044, 2013.

[6] L. Kumar and STAR Collaboration. STAR results from the RHIC beam energy scan-I. *Nuclear Physics A*, 904:256c–263c, 2013.

[7] T. Satogata, L. Ahrens, M. Bai, et al. RHIC challenges for low energy operation. In *Proc. of PAC07*, page 1877, 2007.

[8] A.V. Fedotov, I. Ben-Zvi, X. Chang, et al. Beam dynamics limits for low-energy RHIC operation. In *Proc. of HB2008*, 2008.

[9] A.V. Fedotov, M. Bai, M. Blaskiewicz, et al. Beam lifetime and limitations during low-energy RHIC operation. In *Proc. of PAC11*, 2011.

[10] T. Satogata. RHIC low energy beam loss projections. Technical report, BNL C-A/AP/360, 2009.

[11] C. Montag, T. Satogata, L.A. Ahrens, et al. Experience with low-energy gold-gold operations in RHIC during FY 2010. Technical report, BNL C-A/AP/435, 2011.

[12] C. Montag, P. Thieberger, K. Yip, et al. RHIC performance during the 7.5 GeV low energy run in FY 2014. In *Proc. of IPAC2014*, 2014.

[13] A.V. Fedotov. IBS and potential luminosity improvement for RHIC operation below transition energy. Technical report, BNL C-A/AP/339, 2009.

[14] A.V. Fedotov, I. Ben-Zvi, X. Chang, et al. Feasibility of electron cooling for low-energy RHIC operation. Technical report, BNL C-A/AP/307, 2008.

[15] A.V. Fedotov, M. Blaskiewicz, W. Fischer, et al. Interplay of space-charge and beam-beam effects in a collider. In *Proc. of HB2010*, 2010.

[16] A.V. Fedotov and M. Blaskiewicz. Potential for luminosity improvement for low-energy RHIC operations with long bunches. Technical report, BNL C-A/AP/449, 2012.

[17] A.V. Fedotov, S. Belomestnykh, I. Ben-Zvi, et al. Bunched beam electron cooler for low-energy RHIC operation. In *Proc. of PAC2013*, 2013.

[18] A.V. Fedotov. IBS for RHIC operation below transition energy and various RF systems. Technical report, BNL C-A/AP/477, 2013.

[19] V.L. Litvinenko. Choosing RF system for low energy RHIC operation. Technical report, BNL C-A/AP/476, 2013.

[20] A. Piwinski. Intra-beam scattering. In *Frontiers of Particle Beams*, pages 297–309. Springer, 1988.

[21] A.O. Sidorin, I.N. Meshkov, I.A. Seleznev, et al. BETACOOL program for simulation of beam dynamics in storage rings. *Nuclear Instruments and Methods in Physics Research Section A: Accelerators, Spectrometers, Detectors and Associated Equipment*, 558(1):325–328, 2006.

[22] S. Polizzo. 9 MHz cavity and plans. RHIC retreat 2018, Upton, NY.

[23] A.V. Fedotov, M. Blaskiewicz, W. Fischer, et al. Accelerator physics design requirements and challenges of RF based electron cooler LEReC. In *Proc. of NAPAC16*, 2016.

[24] D. Kayran, Z. Altinbas, D. Bruno, et al. LEReC photocathode DC gun beam test results. In *Proc. of IPAC'18*, pages 1306–1308, 2018.

[25] A.V. Fedotov. Overall goals and things to do. LEReC retreat 2018, Upton, NY.

[26] D. Kayran. Commissioning progress and plans. LEReC retreat 2018, Upton, NY.

[27] K. Schindl. Space charge. In *Beam Measurement*, pages 127–151. World Scientific, 1999.

[28] T. Satogata. RHIC RF harmonic numbers for low energy operations. Technical report, BNL C-A/AP/309, 2008.

[29] C. Liu. Vertex distribution with 9 MHz cavities and comparison of 9 MHz versus 28 MHz cavities for 7.3 GeV operation. Technical report, BNL C-A/AP/612, 2018.

[30] W. Zhang, J. Sandberg, H. Hahn, et al. Research and development of RHIC injection kicker upgrade with nano second FID pulse generator. In *Proc. IPAC2012*, 2012.

[31] C. Gardner. Bucket and bunch parameters for clean injection of low energy gold ions into RHIC. Technical report, BNL C-A/AP/607, 2018.

[32] V. Schoefer. RHIC injection kicker measurement and emittance growth simulation. Technical report, BNL C-A/AP/606, 2018.

[33] E. Keil. Beam-beam dynamics. Technical report, CERN-SL-94-78-AP, 1994.

[34] C. Montag. Recent results on beam-beam effects in space charge dominated colliding ion beams at RHIC. In *Proc. of HB2014*, 2014.

[35] C. Liu. RHIC heavy ion operation with near-integer working point. *submitted to IPAC'19*, 2018.

[36] C. Montag. Multipole error data analysis for RHIC low-energy operations. Technical report, BNL C-A/AP/421, 2011.

[37] W. Fischer, A. Jain, and S. Tepikian. Beam-based measurements of persistent current decay in the Relativistic Heavy Ion Collider. *Physical Review Special Topics-Accelerators and Beams*, 4(4):041002, 2001.

[38] C. Montag, D. Bruno, A. Jain, et al. Mimicking bipolar sextupole power supplies for low-energy operations at RHIC. In *Proc. of PAC2011*, page 2241, 2011.

[39] Thieberger P. Can we demagnetize (”degauss”) the effect of persistent currents in RHIC? RHIC APEX workshop, 2013.

[40] C. Liu. Experimental study of the persistent current in RHIC superconducting dipole. Technical report, BNL C-A/AP/611, 2018.

[41] F. Carlier. Detectors for low energy electron cooling in RHIC. Technical report, BNL C-A/AP/557, 2016.

[42] S.Y. Zhang and M. Blaskiewicz. Recombination monitor. Technical report, BNL C-A/AP/582, 2017.

[43] A. Drees, D. Bruno, T. Curcio, et al. Report on LEReC recombination monitor APEX study June 15th 2016. Technical report, BNL C-A/AP/579, 2016.

[44] F. Carlier, P. Thieberger, W. Fischer, et al. Radiative recombination detection to monitor electron cooling conditions during low energy RHIC operations. In *Proc. of IPAC16*.

[45] K. Zeno. AGS longitudinal emittance measurements for upcoming RHIC low energy gold runs. Technical report, BNL C-A/AP/615, 2018.

[46] W. Fischer et al. RHIC collider projections (FY 2018 –FY 2027). `http://www.rhichome.bnl.gov/RHIC/Runs/RhicProjections.pdf`.